Int J Adv Manuf Technol (2017) 91:3299–3306
DOI 10.1007/s00170-017-0013-y

ORIGINAL ARTICLE

An experimental investigation of grinding force and energy in laser thermal shock-assisted grinding of zirconia ceramics

Sheng Xu[1,2] · **Zhenqiang Yao**[1,2] · **Huangyue Cai**[3] · **Hongyu Wang**[2]

Received: 26 August 2016 / Accepted: 4 January 2017 / Published online: 20 January 2017

Abstract The development of advanced ceramics such as zirconia has gained importance because of their desirable properties. However, the engineering applications of ceramics are still limited by the ability to develop cost-efficient machining techniques. To achieve the cost-efficient production of zirconia parts, laser irradiation was introduced as a step before grinding. In this study, this hybrid process was investigated by measuring the grinding force and the specific grinding energy in grinding tests. The results confirmed significant decreases in the grinding force and specific grinding energy. The decreases suggest that the hybrid process can be an economical and efficient way to overcome the limitation of the high specific energy required for grinding advanced ceramics. Scratch tests were performed to obtain a fundamental understanding of the decreases in the grinding force and energy, and the scratch morphology and crack types beneath the scratch tracks were observed. The transition of crack types and the chip-forming mechanism was confirmed. It was noted that the scratch hardness of ceramics reduced after laser irradiation, which explains the reduction in the grinding force. In addition, micro-debris and lateral cracks were induced by scratching on the surface with laser irradiation, which contributed to the decrease in the specific grinding energy.

Keywords Laser thermal shock-assisted grinding · Advanced ceramics · Grinding force · Specific grinding energy · Material removal mechanism · Scratch

✉ Zhenqiang Yao
zqyaosjtu@gmail.com

Sheng Xu
story2011@sjtu.edu.cn

[1] State Key Laboratory of Mechanical System and Vibration, Shanghai 200240, People's Republic of China

[2] Gas Turbine Research Institute, School of Mechanical Engineering, Shanghai Jiao Tong University, Minhang DistrictShanghai, 200240, People's Republic of China

[3] School of Materials Science and Engineering, Shanghai Jiao Tong University, Shanghai 200240, People's Republic of China

1 Introduction

Advanced ceramic materials such as zirconia, silicon nitride, and alumina possess a unique combination of physical and mechanical properties, which have led to applications in the nuclear industry, the aerospace industry, automotive components, and biocompatible implants [1–3]. However, these properties also create challenges in cost-efficient machining of ceramics parts. Researchers and engineers have worked to confront these challenges, and numerous methods have been developed [4–9]. Recently, a novel laser thermal shock-assisted grinding (LTSG) technique has been developed that offers a promising means for cost-efficient production of ceramic parts. Experimental investigations have been conducted by Kumar et al. to demonstrate the feasibility of LTSG of ceramics [3, 6, 10–12].

This hybrid machining process offers significant advantages over conventional grinding in terms of the grinding force, material removal, and grinding tool life [3, 6, 11]. Kumar [3] reported that the grinding forces associated with LTSG are lower than those associated with conventional grinding under all conditions, with a maximum reduction of 43.2%. In addition, tool wear is lower with LTSG than without it, and higher material removal rates are possible with low grinding forces and low tool wear [3]. Similar results are also reported by Fortunato [6] and Zhang [11]. While these advantages are encouraging, the application domain of LTSG can be

extended to other ceramics, such as commercial zirconia, including partially stabilized zirconia and yttria-stabilized tetragonal zirconia. Zirconia ceramics are used in many high-end applications and have been called "ceramic steel" [13–15] because they have a Young's modulus comparable to that of stainless steel alloys and the highest fracture toughness of any commercial ceramics (as shown in Table 1). These two features have contributed to widespread interest in zirconia as a structural component. Zirconia also has a significantly different microstructure and different physical properties than previously investigated materials such as silicon nitride and alumina ceramics. Silicon nitride contains 5 to 10% glass by weight, whereas commercial zirconia has a negligible glassy phase at the grain boundaries [16]. The grain size of alumina ceramics is usually larger than that of zirconia. Zirconia has an exceptionally high fracture toughness because of the T–M phase transformation. When a T–M transformation takes place, each grain's volume experiences an expansion of approximately 3–4% [15]. The stress field associated with volume dilatation due to phase transformation therefore hinders the propagation of cracks. Toughness is enhanced as a result.

The aforementioned differences in microstructure and physical properties between zirconia and other ceramics result in differences in their grinding characteristics. However, little research has been conducted on the benefits of applying LTSG on zirconia. This study was therefore conducted to examine the grinding characteristics of zirconia during LTSG. The focus of this study was on the grinding force, the specific grinding energy, the surface roughness, and the material reasons for the variation in force and energy by grinding and scratching tests.

2 Material and methods

2.1 Specimens

Fully dense ceramic material was used in this study. The specimens used in the grinding tests were supplied by the Hennai Company (China). Table 1 shows the properties of zirconia, silicon nitride, and alumina at ambient temperature. As the table shows, zirconia has the highest fracture toughness of the three ceramics.

The specimens used in the grinding tests were cut into pieces with L × W × D dimensions of 75 mm × 25 mm × 10 mm. Grinding was performed on the L × W surface. The mean roughness of the surface, R_a, was 0.431 μm.

The specimens used for the scratching tests had L × W × H dimensions of 15 mm × 10 mm × 5 mm. The scratching process was performed on the L × W surface, which was polished, and the mean roughness of the specimens, R_a, was 0.015 μm.

2.2 Laser irradiation procedure (Fig. 1)

Laser irradiation was conducted using an IPG fiber laser. The thickness of the heat-affected layer can be controlled by adjusting the laser power, spot size, and speed [3]. In the current study, the power of the laser beam was 190 W, and the laser scan speed was 60 mm/s. The diameter of the laser spot was approximately 5 mm, and the distance between the two laser tracks was 3 mm. Before laser irradiation, a layer of carbon powder was sprayed on the specimen's surface to improve the laser absorption.

2.3 Grinding procedure

Surface grinding was conducted using a high-speed grinding machine (BLOHM). A vitrified bond diamond wheel (Saint–Gobain Abrasives, Germany) was employed. The size of the diamond grit was approximately 120 μm. The diameter of the wheel was 400 mm, and the rim width was 10 mm. Before grinding, the wheel was balanced using a dynamic balancing instrument (Shanghai Ringod Tech. & Trad. Co., Ltd., China). The peripheral wheel speed (V_s) and the worktable speed (V_w) were constant while the depth of cut (a_p) was varied in the grinding tests, as shown in Table 2.

The normal and tangential grinding forces, F_n and F_t, were measured using a dynamometer. To obtain reliable values for the grinding forces, every set of grinding tests with the same grinding parameters was conducted at least three times, and the mean values were calculated and recorded.

In the grinding experiments, no cross feed was provided, and no spark-out or further surface treatment was conducted. After being ground, the specimens were cleaned in acetone for 5 min using an ultrasonic washer. Next, the roughness of the

Table 1 Thermal and mechanical properties of ceramics at room temperature

	Zirconia [17]	Silicon nitride [16, 18]	Alumina [19]
Elastic modulus (GPa)	210	306	300
Fracture toughness (MPa-$m^{1/2}$)	8–13	4.2–7.0	4–5
Density (g/cm^3)	6.02	3.22	3.72
Thermal expansion coefficient (10^{-6}/K)	10.3	3.1	8.2
Thermal conductivity (W/m K)	2.2	17.6	35
Specific heat (J/kg K)	450	642	880

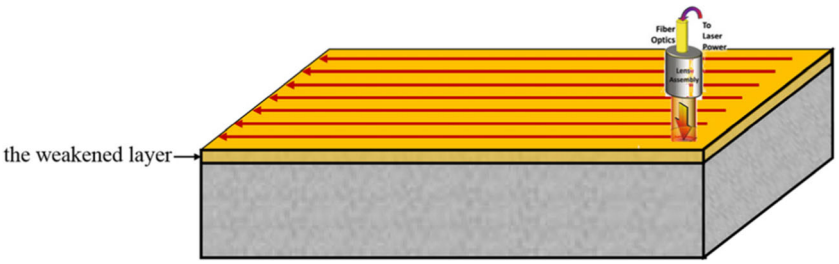

Fig. 1 Illustration of the irradiation experimental setup and processing (the material is zirconia, and the orange layer is the heat-affected/weakened layer)

surface was measured across the grinding direction using a profilometer (SJ-210, Mitutoyo Corporation, Japan) with a cut-off length of 0.8 mm and an evaluation length of 4 mm (in accordance with ISO 4287:1997).

3 Experimental results

3.1 Grinding forces (Fig. 2)

Each specimen was fixed on the dynamometer using a special fixture, and the down grinding mode was employed. Every grinding pass started from the left edge of the specimen and removed material with a depth a_p. The grinding wheel was then raised, returned to the left edge, and started on the next grinding pass. The forces generated in every grinding pass were recorded and are illustrated in Fig. 3. Every point in Fig. 3 is the average value obtained from at least three repeated tests, and the error bar represents the range of the values.

The results shown in Fig. 3 indicate that the normal grinding force decreased significantly after laser irradiation of the specimen. When 5 μm was adopted as the depth of cut (a_p), the minimum value of the average grinding force was 35.53 N. The normal force increased with increasing grinding circle. The reason for the increase in force is that the effect of laser irradiation on the material becomes weaker with increasing depth from the original surface. When the heat-affected layer produced by laser irradiation is removed completely, the grinding force stabilized to an asymptotic value of approximately 48 N. For comparison, experiments were conducted on a non-laser-irradiated workpiece, and the average force was 48.5 N, which approximates the asymptotic value of the grinding force on workpieces subjected to laser irradiation. These results confirmed that laser irradiation on the ceramic specimens resulted in a reduction in grinding force and that the magnitude of the reduction was approximately 26.0% for a depth of cut of 5 μm. When the depth of cut was 10 μm, the minimum value and asymptotic values were 48.3 and 74 N, respectively. The variation in the grinding force was approximately 34.7%. The average grinding force on a comparable non-laser-irradiated workpiece was 74.3 N. When the depth of cut was 20 μm, the minimum value and asymptotic values were 94.8 and 121 N, respectively. The variation in the grinding force was approximately 21.7%. The average grinding force on a comparable non-laser-irradiated workpiece was 121.2 N. As the above results show, the variation in grinding force was greatest when the depth of cut was 10 μm.

In the grinding process, sharp grit becomes dull through attrition wear when the grit interacts with the workpiece. A larger grinding force can accelerate the wear process. At the same time, the grinding force becomes larger with dulling of the abrasive grit. When the grinding force is sufficiently large, this grit will separate from the grinding wheel. Therefore, a reduction in grinding force is desirable because a smaller grinding force per unit volume of material removal results in a longer wheel life and lower wheel cost. The wheel cost is an important factor when grinding with diamond wheels; therefore, any reduction in wheel consumption is directly reflected in a lower grinding cost [20]. The cost associated with the grinding process has been a major factor that has hindered ceramics applications [21].

The error bars are large at the beginnings of the curves shown in Fig. 3 and small at the ends of the curves. Large error bars mean that the grinding force varies greatly during grinding of laser-irradiated surfaces while small error bars mean that the grinding force is more stable during grinding of the unaffected parent material. The variation in force is caused by chips fracturing off from the surface. Thus, a large variation in the grinding force represents an increase in the brittleness of the material. This can be beneficial for zirconia ceramics because the penetration depth of subsurface damage decreases with increasing in ceramic brittleness in a brittle grinding mode [22].

3.2 Specific grinding energy

The specific grinding energy is defined as the energy consumed per unit volume of material removed. It is one of the

Table 2 Parameters of grinding experiments

	Set 1	Set 2	Set 3
Peripheral wheel speed V_s (m/s)	30	30	30
Worktable speed V_w (m/min)	1	1	1
Depth of cut a_p (μm)	5	10	20

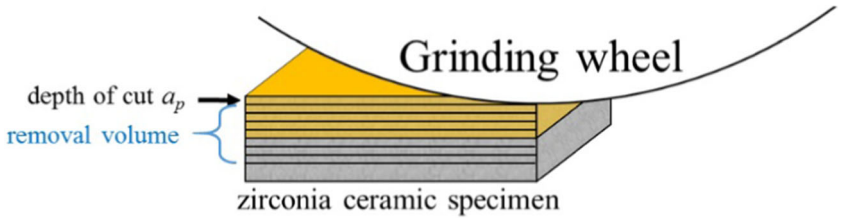

Fig. 2 Illustration of the grinding experimental setup and processing

most important performance parameters in the grinding process and is dependent on the workpiece material and grinding conditions. Under the same grinding conditions, a large specific grinding energy means that the material is difficult to remove, which is undesirable because it results in high material removal costs [23]. The specific grinding energy can be calculated as follows:

$$u = \frac{V_s}{bV_w a_p} F_t$$

where u is the specific grinding energy, F_t is the tangential grinding force, V_s is the peripheral wheel speed, b is the rim width, V_w is the worktable speed, and a_p is the depth of cut. The specific grinding energy results obtained from the grinding tests are shown in Fig. 4.

It was noted that laser irradiation can lead to a substantial decrease in the specific grinding energy. This decrease has great significance for ceramic grinding because the high specific energy required for grinding advanced ceramics is one of the limiting factors in the industrial utility of ceramics [23]. The specific grinding energy results obtained in this study suggest that laser irradiation can be an economical and efficient way to overcome this limitation. According to Fig. 4, the specific grinding energy was 105.6 J/mm^3 when grinding was performed on an irradiated surface with a depth of a_p = 5 μm. The specific grinding energy increased as the heat-affected layer was removed. When the heat-affected layer produced by laser irradiation was removed completely, the specific grinding energy stabilized at approximately 125 J/mm^3. The magnitude of the reduction in the specific grinding energy was approximately 15.5% after laser irradiation. For depths of cut of a_p = 10 μm and a_p = 20 μm, the magnitudes of the reduction were 43.61 and 31.76%, respectively. As with the grinding force, the greatest reduction in the specific grinding energy was observed when the depth of cut was 10 μm. The reason for this may be that the grinding conditions of v_s = 30 m/s, v_w = 1 m/min, and a_p = 10 μm approximated the critical conditions of the brittle–ductile transition during grinding. In addition, laser irradiation may cause the brittle–ductile transition to occur sooner. In other words, the variation in the proportion of the plow during the grinding process may be larger when a_p = 10 μm than when a_p = 5 μm. Thus, the reductions in the specific grinding energy and grinding force would be greater for a_p = *10* μm than for a_p = *5* μm. When the depth of cut increased to 20 μm, the number of flaws per unit volume of material removed decreased, so the reductions in the specific grinding energy and grinding force were smaller for a_p = 20 μm than for a_p = 10 μm.

The turn points of all of the specific grinding energy curves are approximately 40 μm. That is, the heat-affected layer caused by laser irradiation was removed completely when the material removal depth reached 40 μm, and the material ground subsequently was unaffected parent material.

A second result that can be drawn from Fig. 4 is that increasing the depth of cut (a_p) can reduce the specific grinding energy. This finding is confirmed by many investigators. In this study, the stable specific grinding energy values were 125, 105, and 76.5 J/mm^3 for a_p = 5, 10, and 20 μm, respectively.

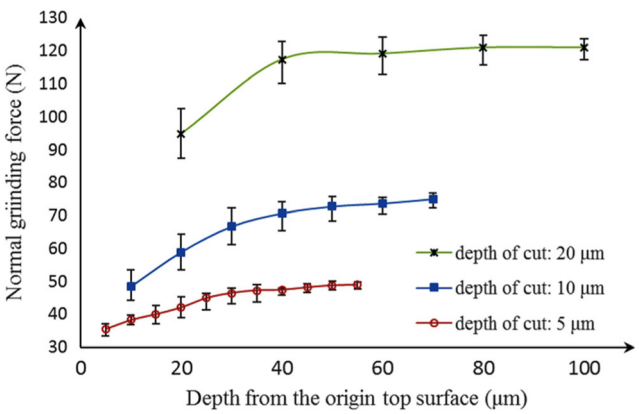

Fig. 3 Normal grinding force vs. depth from the original surface

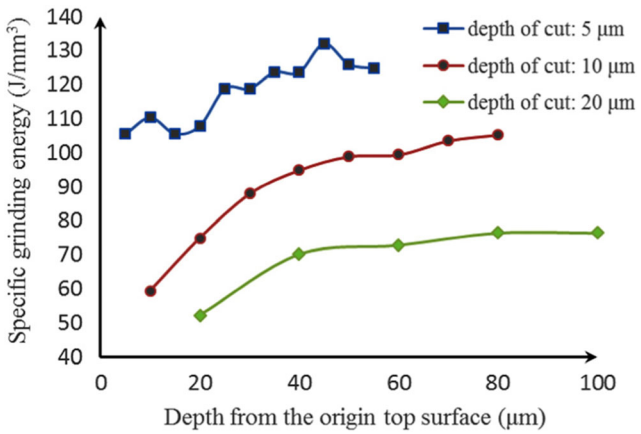

Fig. 4 Specific grinding energy vs. depth from the original surface

However, the thickness of the damaged layer introduced by grinding increases as the depth of cut increases. Especially, the risk is greater for less brittle ceramics (such as zirconia ceramics) because they tend to have more clustered microcracks and are much more susceptible to abrupt strength loss [24, 25]. This risk may be reduced by irradiating the surface of less brittle ceramics with a laser, as discussed further in Sect. 4.2.

3.3 Surface roughness and morphology

The roughness across the grinding direction was measured after the first grinding pass and last grinding pass in each grinding test. The results are shown in Fig. 5. The blue bars indicate values measured after the first grinding pass, and the green bars indicate values measured after the last grinding pass. An abnormal phenomenon was observed in the results for a_p = 5 μm: the roughness after the first cut, as indicated by bar (a) in Fig. 5, was greater than that for a_p = 10 and 20 μm, as indicated by bars (c) and (e), respectively. The reason for this may be that more flaws per unit volume are left on the surface when the depth of cut is 5 μm. In other words, may laser irradiation worsen the surface roughness during the first grinding pass. However, this effect can be eliminated by removing the heat-affected layer completely, as the green bars in Fig. 5 show. Therefore, laser irradiation has little effect on the surface roughness.

4 Discussion

To determine why the grinding force and the specific grinding energy decrease and to identify the material removal mechanism, scratch tests were conducted on the ceramic surfaces. The grinding process is the result of individual pieces of abrasive grit engaging in cutting action. Thus, investigations into the grinding process are primarily based on a single-abrasive scratch process that saves the study from being distracted by abrasive–abrasive interaction during grinding, although the scratch speed is lower than the peripheral grinding wheel speed [12, 26].

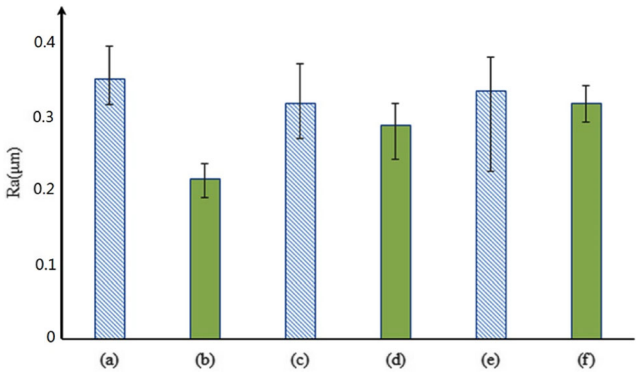

Fig. 5 Roughness measured across the grinding direction after the first cut and last cut in each grinding test. **a** a_p = 5 μm, after the first cut. **b** a_p = 5 μm, after the last cut. **c** a_p = 10 μm, after the first cut. **d** a_p = 10 μm, after the last cut. **e** a_p = 20 μm, after the first cut. **f** a_p = 20 μm, after the last cut

4.1 Surface morphology of scratching and material removal mechanism

Before the scratch tests, the maximum undeformed chip thickness that can be produced by an individual piece of abrasive grit during grinding should be calculated, and the scratch depth should be on the order of the maximum undeformed chip thickness.

The maximum undeformed chip thickness can be calculated as follows: [1, 27]

$$h_{\max} = \left[\frac{3}{C\ \tan\theta}\ \frac{V_w}{V_s}\ \sqrt{\frac{a_p}{d_s}}\right]^{1/2}$$

where h_{max} is the maximum undeformed chip thickness, C is the active grit density, θ is the semi-included angle of the active grit point (θ = 60° is often used), V_s is the peripheral wheel speed, V_w is the worktable speed, a_p is the depth of cut, and d_s is the diameter of the wheel. In the current study, C was taken to be 18 grits/mm^2, based on information provided by the manufacturer of the grinding wheel. The calculated values of the maximum undeformed chip thickness are shown in Table 3. A load of 200 mN was adopted to make the scratch depth comparable to the maximum undeformed chip thickness. The scratch tests were performed using a Nano Indenter XP (Agilent Technologies, Inc., USA).

A Berkovich indenter was employed because the scratch process achieved with a rough indenter is comparable to the grinding process [18, 28]. The scratch results are shown in Fig. 6. The scratch tracks are located between the yellow lines.

Scanning electron microscopy (SEM) micrographs of the scratch tracks are shown in Fig. 6. As Fig. 6a shows, the tracks on the surface without laser irradiation are smooth, which strongly suggests that the plasticity of zirconia ceramic is excellent before it is irradiated. Furthermore, no ruffle is observable, which confirms that the scratch process is stable on the surface. This explains the phenomenon of the error bars being short at

Table 3 Maximum undeformed chip thicknesses

h_{max}	a_p	V_s	V_w
0.4350 μm	5 μm	30 m/s	1000 mm/min
0.5173 μm	10 μm	30 m/s	1000 mm/min
0.6152 μm	20 μm	30 m/s	1000 mm/min

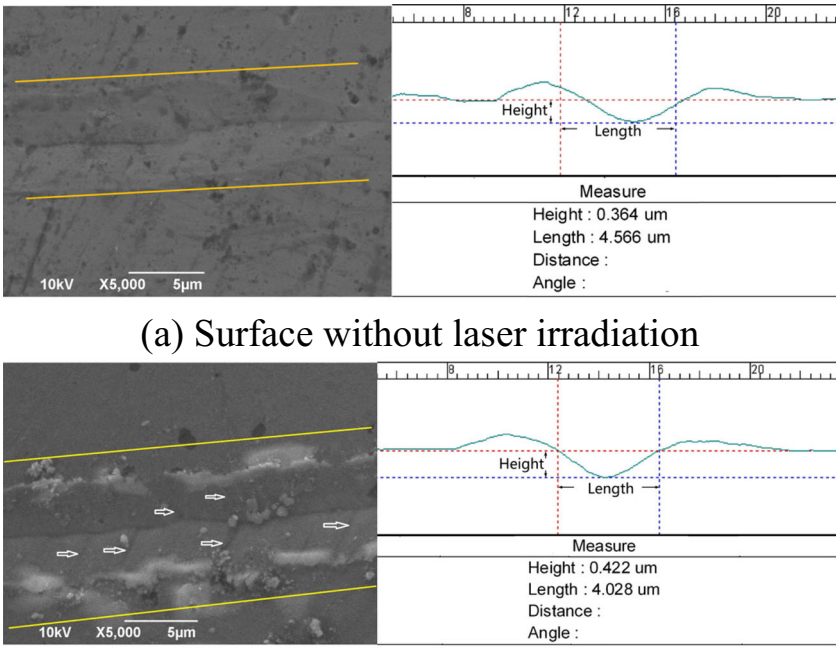

Fig. 6 SEM observation of scratch tracks on surfaces with and without laser irradiation

the ends of the curves in Fig. 3. These results indicate that the plow forms a major proportion of the scratch process.

Figure 6b shows that some debris emerges around the edge of the scratch track on the surface with laser irradiation, and ruffles (indicated by white arrows) are observable on the surfaces of the tracks. This debris indicates that the proportion of cutting that occurs during the scratch process becomes greater. Furthermore, this debris indicates that the material removal mechanism is pulverization. In pulverization, a tortuous crack that is about to cleave the grain into several pieces is arrested at the grain boundaries that hinder further propagation of the crack into the surrounding grains [25]. The transition of the material removal mechanism can cause the specific grinding energy to decrease significantly [1], and the reason for this reduction is that the proportion of the plow decreases and the proportion of cutting increases during the grinding process.

For a normal scratch load of 200 mN, the depth of the tracks on the surface without laser irradiation was 0.36 μm, whereas the depth of the tracks on the surface with laser irradiation was 0.42 μm. This increase in the depth indicates a decrease in the scratch hardness, which is defined as the normal force applied over the projected area of contact on a plane perpendicular to the motion of the indenter. In other words, the surface is more easily penetrated by abrasive grit during grinding of ceramics. This conclusion was confirmed by checking the Vickers hardness of the surfaces with and without laser irradiation. The average values of the Vickers hardness were 1156.4 HV with laser irradiation and 1240.7 HV without laser irradiation. The decrease in hardness achieved by laser irradiation can reduce the normal grinding force [29], as confirmed by the results reported in Sect. 3.1. This is an advantage in overcoming a major obstacle in the grinding of ceramics—a large normal grinding force prevents the material removal rate from being increased because a large normal force can cause severe median/radial cracks. Zirconia ceramics in particular tend to have more clustered microcracks than some other types of ceramics and are much more susceptible to abrupt strength loss because of their less brittle nature. A reduction in the normal grinding force contributes to decreasing the risks of large radial cracks and abrupt strength loss.

4.2 Subsurface crack types and material removal mechanism

The behavior of a single grit during grinding was simulated by scratching specimen surfaces, as described in Sect. 4.1 and observing the microchips formed. However, it cannot be determined from this type of testing that the microchips are caused by interactions between radial/median cracks or between lateral cracks, because the Berkovich indenter is a type of sharp indenter that causes material removal (and vanishing of cracks) during scratch tests. This is a disadvantage in determining the crack type and answering the question of how the material is separated from the surface. To answer these questions, cracks produced in large-load scratch tests, conducted using a conical diamond indenter with a load of 100 N, were examined in this study. No material was removed

during the scratching, and the cracks caused by the scratching were preserved completely in the scratch tests.

After the scratch tests, each specimen was cut into two pieces, and the distance between the end of each scratch track and the cut line was set to be greater than 100 μm to avoid the effect of cutting on the subsurface cracks beneath the scratch track. Next, the surface of each piece was polished. Micrographs of the subsurface damage beneath the scratch tracks are shown in Fig. 7.

The most important information obtained from Fig. 7 is the change in the crack type associated with subsurface damage. As Fig. 7 shows, there is only a lateral crack beneath the scratch tracks on the surface with laser irradiation, while only median/radial cracks can be observed beneath the scratch tracks on the surface without laser irradiation. That is to say, the crack type caused by grinding can be changed from median/radial cracks to lateral cracks by irradiating the ceramic surface. The reasons for this change may be that the heat-affected layer is sensitive to the propagation of cracks and that cracks tend to develop in this layer and not in the direction of depth. This phenomenon is very important in ceramic grinding because lateral cracks are touted as controlling material removal in brittle materials and because median/radial cracks diminish the strength of ceramics [30, 31]. In other words, when lateral cracks are generated with little or no median/radial cracking occurring during processing, material removal can be accomplished with less damage. This phenomenon is desirable in relatively rough grinding because the change may solve the problem, identified by Lee et al., of zirconia ceramics losing strength catastrophically under severe grinding conditions [24]. Because of the decrease in the risk of abrupt strength loss, the material removal rate in relatively rough grinding can be increased significantly. The thickness of the damage caused by abrasion can be reduced significantly by irradiating the surface of zirconia ceramics, as Fig. 7 shows. This is an exciting result for ceramic grinding. In the future, we intend to focus on modeling the depth of the damage, based on statistical analysis of grinding test results.

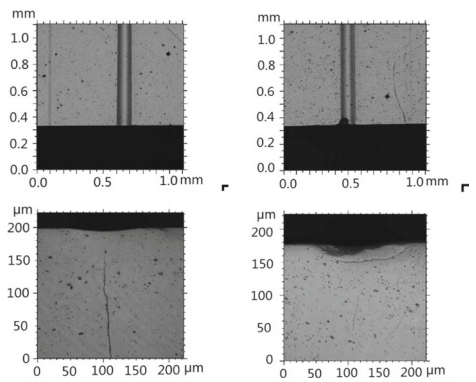

(a) surface without laser irradiation (b) surface with laser irradiation

Fig. 7 Micrographs of scratch tracks and subsurface cracks

5 Conclusions

To study the grinding characteristics of LTSG in terms of the grinding force, grinding specific energy, and surface roughness, grinding tests were conducted on the surfaces of ceramics with and without laser irradiation. Scratch tests were also performed to provide a basis for understanding the variations in the grinding force and specific surface energy, the material removal mechanism, and the types of cracks that occur in LTSG ceramics.

Laser irradiation on the surfaces of ceramics can decrease the grinding force significantly. In this study, the grinding force varied more during grinding of the heat-affected layer than during grinding of the unaffected parent material. The specific grinding energy was also reduced significantly by irradiating the surface of zirconia. The variation in the grinding force was greatest when the depth of cut was 10 μm. The thickness of the heat-affected layer was approximately 40 μm. Laser irradiation worsens the surface roughness created by the first grinding pass. However, this adverse effect can be eliminated by removing the heat-affected layer completely. These grinding test results suggest that laser irradiation before grinding can be an economical and efficient way to overcome the limitations posed by the high grinding force and energy required to grind ceramics.

The reasons for the decreases in the grinding force and the specific grinding energy are discussed and explained in this paper on the basis of the results of scratch tests. The grinding force decreases because the scratch hardness decreases and the brittleness of zirconia increases after laser irradiation. The specific grinding energy decreases because of a combination of the transition of the material removal mechanism and a change in crack type produced during the grinding process. The increase in brittleness of the heat-affected layer can contribute to decreasing the risks of large radial cracks and abrupt strength loss. In addition, laser irradiation decreases the depth of the scratch damage on the surface. This is an exciting result for ceramic grinding and should be studied further.

This study also produced some interesting results concerning the types of cracks produced beneath scratch tracks. Additional research will be conducted on the subsurface damage produced in ceramics by LTSG.

Acknowledgments This research was financially supported by the National Natural Science Foundation of China (Grant No. 51475299) and the State Key Laboratory of Mechanical System and Vibration (Grant No. MSVZD201412) and the National Natural Science Foundation of China (Grant No. 61403352). The authors are grateful to the editors and reviewers who made constructive comments.

References

1. Chen J, Shen J, Huang H, Xu X (2010) Grinding characteristics in high speed grinding of engineering ceramics with brazed diamond wheels. J Mater Process Technol 210(6):899–906
2. Agarwal S, Rao PV (2008) Experimental investigation of surface/subsurface damage formation and material removal mechanisms in SiC grinding. Int J Mach Tools Manuf 48(6):698–710
3. Kumar M, Melkote S, Lahoti G (2011) Laser-assisted microgrinding of ceramics. CIRP Annals-Manufacturing Technology 60(1):367–370
4. Rabiey M, Jochum N, Kuster F (2013) High performance grinding of zirconium oxide (ZrO 2) using hybrid bond diamond tools. CIRP Annals-Manufacturing Technology 62(1):343–346
5. Tang H, Deng Z, Guo Y, Qian J, Reynaerts D (2015) Depth-of-cut errors in ELID surface grinding of zirconia-based ceramics. Int J Mach Tools Manuf 88:34–41
6. Fortunato A, Guerrini G, Melkote SN, Bruzzone AA (2015) A laser assisted hybrid process chain for high removal rate machining of sintered silicon nitride. CIRP Annals-Manufacturing Technology 64(1):189–192
7. Liang Z, Wang X, Wu Y, Xie L, Jiao L, Zhao W (2013) Experimental study on brittle–ductile transition in elliptical ultrasonic assisted grinding (EUAG) of monocrystal sapphire using single diamond abrasive grain. Int J Mach Tools Manuf 71:41–51
8. Zhong Z, Venkatesh V (2009) Recent developments in grinding of advanced materials. Int J Adv Manuf Technol 41(5–6):468–480
9. Shen X, Lei S (2011) Experimental study on operating temperature in laser-assisted milling of silicon nitride ceramics. Int J Adv Manuf Technol 52(1–4):143–154
10. Zhang X, Chen G, An W, Deng Z, Liu W, Yang C (2014) Experimental study of machining characteristics in laser induced wet grinding silicon nitride. Mater Manuf Process 29(11–12):1477–1482
11. Zhang X, Chen G, An W, Deng Z, Zhou Z (2014) Experimental investigations of machining characteristics of laser-induced thermal cracking in alumina ceramic wet grinding. Int J Adv Manuf Technol 72(9–12):1325–1331
12. Xu S, Yao Z, Zhang M (2016) Material removal behavior in scratching of zirconia ceramic surface treated with laser thermal shock. Int J Adv Manuf Technol 85(9):2693–2701. doi:10.1007/s00170-015-8098-7
13. Manicone PF, Iommetti PR, Raffaelli L (2007) An overview of zirconia ceramics: basic properties and clinical applications. J Dent 35(11):819–826
14. Garvie R, Hannink R, Pascoe R (1975) Ceramic steel? Nature 258(5537):703–704
15. Piconi C, Maccauro G (1999) Zirconia as a ceramic biomaterial. Biomaterials 20(1):1–25
16. Pfefferkorn FE, Shin YC, Tian Y, Incropera FP (2004) Laser-assisted machining of magnesia-partially-stabilized zirconia. J Manuf Sci Eng 126(1):42–51
17. Huang H (2003) Machining characteristics and surface integrity of yttria stabilized tetragonal zirconia in high speed deep grinding. Mater Sci Eng A 345(1):155–163
18. Desa O, Bahadur S (1999) Material removal and subsurface damage studies in dry and lubricated single-point scratch tests on alumina and silicon nitride. Wear 225:1264–1275
19. Yan Y, Li L, Sezer K, Whitehead D, Ji L, Bao Y, Jiang Y (2011) Experimental and theoretical investigation of fibre laser crack-free cutting of thick-section alumina. Int J Mach Tools Manuf 51(12):859–870
20. Hwang T, Evans C, Whitenton E, Malkin S (2000) High speed grinding of silicon nitride with electroplated diamond wheels, part 1: wear and wheel life. J Manuf Sci Eng 122(1):32–41
21. Xie G, Huang H (2008) An experimental investigation of temperature in high speed deep grinding of partially stabilized zirconia. Int J Mach Tools Manuf 48(14):1562–1568
22. Zhang B, Howes TD (1995) Subsurface evaluation of ground ceramics. CIRP Annals-Manufacturing Technology 44(1):263–266
23. Singh V, Rao PV, Ghosh S (2012) Development of specific grinding energy model. Int J Mach Tools Manuf 60:1–13
24. Kun Lee S, Tandon R, Readey MJ, Lawn BR (2000) Scratch damage in zirconia ceramics. J Am Ceram Soc 83(6):1428–1432
25. Zhang B, Zheng X, Tokura H, Yoshikawa M (2003) Grinding induced damage in ceramics. J Mater Process Technol 132(1):353–364
26. Zhang C, Feng P, Zhang J (2013) Ultrasonic vibration-assisted scratch-induced characteristics of C-plane sapphire with a spherical indenter. Int J Mach Tools Manuf 64:38–48
27. Malkin S (1989) Grinding technology: theory and applications of machining with abrasives, 1989. Society of manufacturing engineers, Dearborn, Michigan
28. Sivakumar R, Jones MI, Hirao K, Kanematsu W (2006) Scratch behavior of SiAlON ceramics. J Eur Ceram Soc 26(3):351–359
29. Agarwal S, Rao PV (2013) Predictive modeling of force and power based on a new analytical undeformed chip thickness model in ceramic grinding. Int J Mach Tools Manuf 65:68–78
30. Cook RF, Pharr GM (1990) Direct observation and analysis of indentation cracking in glasses and ceramics. J Am Ceram Soc 73(4):787–817
31. Gu W, Yao Z, Li H (2011) Investigation of grinding modes in horizontal surface grinding of optical glass BK7. J Mater Process Technol 211(10):1629–1636